

Cite this: *Chem. Sci.*, 2021, 12, 14494

All publication charges for this article have been paid for by the Royal Society of Chemistry

Received 10th August 2021
Accepted 8th October 2021

DOI: 10.1039/d1sc04369b

rsc.li/chemical-science

Visible light-induced oxidative *N*-dealkylation of alkylamines by a luminescent osmium(vi) nitrido complex†Jing Xiang,^{a*} Min Peng,^a Yi Pan,^b Li-Juan Luo,^a Shun-Cheung Cheng,^b Xin-Xin Jin,^a Shek-Man Yiu,^b Wai-Lun Man,^c Chi-Chiu Ko,^b Kai-Chung Lau^{b*} and Tai-Chu Lau^{b*}

N-Dealkylation of amines by metal oxo intermediates (M=O) is related to drug detoxification and DNA repair in biological systems. In this study, we report the first example of *N*-dealkylation of various alkylamines by a luminescent osmium(vi) nitrido complex induced by visible light.

High-valent metal oxo (M=O) species play key roles in many chemical and biological oxidation processes.¹ They are versatile oxidants that can perform oxidation of substrates *via* a variety of pathways, including electron transfer, H-atom transfer, hydride transfer and O-atom transfer. In principle, high-valent metal nitrido (M≡N) complexes should also function as versatile oxidants similar to M=O. Although there have been significant advances in M≡N oxidation chemistry in recent years, the reactivity of M≡N is still rather limited in scope compared to M=O.² M≡N is intrinsically less oxidizing than M=O due to the stronger electron donating property of the N³⁻ ligand than the O²⁻ ligand. Attempts to increase the oxidizing power of M≡N by increasing the oxidation state or by using less electron-donating ancillary ligands often led to decomposition of the complexes, mainly due to facile coupling of the nitrido ligands to yield N₂ (2M≡N → 2M + N₂).³ One appealing strategy to enhance the reactivity of M≡N is photochemical excitation. We have recently designed an osmium(vi) nitrido complex [Os^{VI}(N)(L)(CN)₃]⁻ (NO₂-OsN, HL = 2-(2-hydroxy-5-nitrophenyl) benzoxazole) that is strongly luminescent in the solid state and in fluid solutions.⁴ It readily absorbs visible light to generate a long-lived and highly oxidizing excited state with a redox potential of *ca.* 1.4 V. The excited state of this complex also possesses [Os=N[•]] nitridyl characteristics that enable it to readily abstract H-atoms from inert organic substrates.⁵

We report herein the visible-light induced *N*-dealkylation of various alkylamines by NO₂-OsN. Iron oxo species have been used by heme and nonheme enzymes to carry out *N*-dealkylation reactions of tertiary amines, which are important processes involved in detoxification and DNA repair.⁶ A number of synthetic iron(IV) oxo complexes are also able to carry out such *N*-dealkylation reactions.⁷ Mechanistic studies using cytochrome P₄₅₀ and synthetic iron oxo complexes indicate that there are two possible mechanisms for *N*-dealkylation of amines, namely hydrogen-atom transfer (HAT) and electron transfer–proton transfer (ET-PT) (Fig. 1).⁸ In this work we report the first example of *N*-dealkylation of various aromatic as well as aliphatic tertiary amines by a nitrido complex upon visible light excitation. We also provide unambiguous evidence that these reactions occur *via* an ET/PT mechanism.

N-Dealkylation of amines

The reactions of NO₂-OsN with various amines are summarized in Fig. 2. The reaction with *N,N*-dimethylaniline (DMA) is described in detail. Upon irradiation with blue light ($\lambda > 460$ nm), the light-yellow solution containing NO₂-OsN and 10

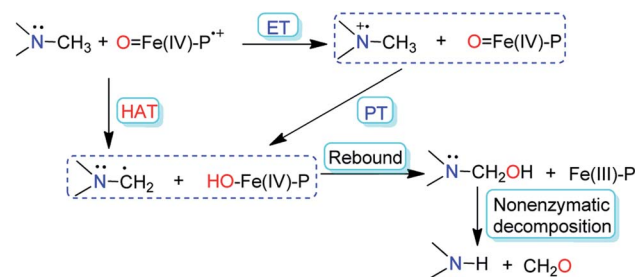


Fig. 1 Two possible mechanisms for *N*-demethylation of tertiary amines by cytochrome P₄₅₀ and synthetic Fe(IV) oxo complexes (P = porphyrin).

^aCollege of Chemistry and Environmental Engineering, Yangtze University, Jingzhou 434020, Hubei, P. R. China. E-mail: xiangjing@yangtzeu.edu.cn

^bDepartment of Chemistry, City University of Hong Kong, Tat Chee Avenue, Kowloon Tong, Hong Kong, China. E-mail: bhtclau@cityu.edu.hk; kaichung@cityu.edu.hk

^cDepartment of Chemistry, Hong Kong Baptist University, Kowloon Tong, Hong Kong 999077, People's Republic of China

† Electronic supplementary information (ESI) available. CCDC 2083709–2083711. For ESI and crystallographic data in CIF or other electronic format see DOI: 10.1039/d1sc04369b



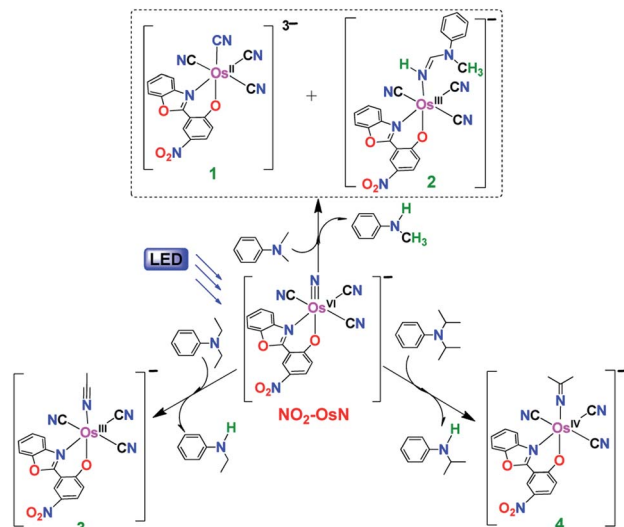


Fig. 2 The photoreactions of $\text{NO}_2\text{-OsN}^*$ with various amines.

equiv. of DMA in CH_2Cl_2 gradually turned red. Analysis of the product solution by GC/MS and GC/FID reviewed the formation of *N*-methylaniline in 71% yield (based on $\text{NO}_2\text{-OsN}$ consumed) (Table S1†), indicating that *N*-demethylation of DMA has occurred. The fate of the fragmented methyl group and the nature of the osmium product(s) were investigated by ESI/MS (Fig. S1†). The ESI/MS of the product solution exhibits a predominant peak at m/z 275.6, which can be assigned to $[\text{Os}(\text{L})(\text{CN})_4]^{2-}$, and this peak shifted to m/z 276.1 when the ^{15}N -labeled nitrido complex ($\text{NO}_2\text{-Os}^{15}\text{N}$) was used, indicating that the extra CN^- is derived from the addition of the fragmented CH_3 group to the nitrido ligand, followed by internal redox (see the Proposed mechanism section below). The ESI/MS also shows a major peak at m/z 659, which is assigned to the amidine product $[\text{Os}(\text{L})(\text{CN})_3(\text{NH}=\text{DMA}_{(-2\text{H}})]^-$ (2), see Fig. S1†.

An attempt to isolate complex 1 by extracting the product residue with H_2O followed by the addition of PPh_4Cl resulted in a PPh_4^+ salt of $[\text{Os}^{\text{II}}(\text{L})(\text{CN})_4]^{3-}$ (1) mixed with a small amount of $[\text{Os}^{\text{III}}(\text{L})(\text{CN})_4]^{2-}$ (1'). However, pure $(\text{PPh}_4)_2\text{1}'$ could be isolated as a dark red microcrystalline solid in ca. 68% yield by slow evaporation of a $\text{MeOH}/\text{H}_2\text{O}$ solution of the mixture under air. Both 1 and 1' show the same peak at m/z 275.6 in ESI/MS. On the other hand, complex 2 could be readily separated from the reaction mixture by column chromatography and isolated as the PPh_4^+ or $^n\text{Bu}_4\text{N}^+$ salt in ca. 16% yield. $(\text{PPh}_4)_2\text{1}'$ and $(\text{PPh}_4)_2$ were characterized by IR, UV/vis, cyclic voltammetry (CV) and ESI/MS (Fig. S2–S6†). The IR spectrum of 1' shows three $\nu(\text{C}\equiv\text{N})$ stretches at 2085, 2038 and 1995 cm^{-1} , while that of 2 shows two $\nu(\text{C}\equiv\text{N})$ stretches at 2113 and 2088 cm^{-1} .

N-Dealkylation also occurs in the reactions of $\text{NO}_2\text{-OsN}^*$ with *N,N*-diethylaniline (DEA) and *N,N*-diisopropylaniline (DPA), resulting in 87% of *N*-ethylaniline and 91% of *N*-isopropylaniline, respectively. Similar to the case of DMA, the fragmented alkyl groups in DEA and DPA are attached to the nitrido ligand, followed by internal redox to give $[\text{Os}^{\text{III}}(\text{L})(\text{CN})_3(\text{N}\equiv\text{C}(\text{CH}_3)_2)]^-$ (3) and $[\text{Os}^{\text{IV}}(\text{L})(\text{CN})_3(\text{N}=\text{C}(\text{CH}_3)_2)]^-$ (4), respectively. 3 and 4 were

isolated as the PPh_4^+ salts in 80% and 82% yields, respectively, and they were characterized by IR, UV/vis, ESI/MS and ^1H NMR (Fig. S7–S9†). Besides the aromatic tertiary amines, dealkylation of the aliphatic tertiary amine Et_3N by $\text{NO}_2\text{-OsN}^*$ was also found, with diethylamine formed in 72% yield. In contrast to the case of DMA, <2% of amidine products were found for DEA and Et_3N reactions, while no amidine product was found for DPA reaction. The UV/vis and ESI/MS collected at various time intervals for these photochemical reactions are summarized in Fig. S10 and S11.†

The molecular structures of $(^n\text{Bu}_4\text{N})_2$, $(\text{PPh}_4)_3$ and $(\text{PPh}_4)_4$ were determined by X-ray crystallography. As shown in Fig. 3a, the Os center in 2 is 6-coordinated by three CN^- ligands, a bidentate O^-N ligand and a neutral amidine ligand in a distorted octahedral geometry. The Os–N6 bond length is 2.048(4) Å and the Os–N6–C17 bond angle is 126.3(3)°, consistent with a neutral amidine ligand. The C17–N6 (1.276(6) Å) and C17–N7 (1.338(6) Å) bond distances, and the N6–C17–N7 bond angle (127.8(5)°) are similar to those of reported amidine complexes.⁹ In 3, the Os–N5 and N5–C17 bond lengths of 2.017(4) and 1.135(7) Å, respectively, and the close to linear Os1–N5–C17 bond angle of 172.0(4)° are consistent with a neutral CH_3CN ligand. Complex 4 features an anionic iminato ligand; the Os–N5 bond length is 1.849(9) Å, indicating a double bond character. The C5–N17 bond is 1.187(13) Å, typical of the $\text{C}=\text{N}$ double bond.

Quenching of the excited state of $\text{NO}_2\text{-OsN}$ by *N,N*-dimethylaniline (DMA) and *N,N*-diethylaniline (DEA) in CH_2Cl_2 was investigated. The bimolecular quenching rate constants (k_q) obtained from Stern–Volmer plots are $(8.5 \pm 0.1) \times 10^9 \text{ M}^{-1} \text{ s}^{-1}$ and $(9.2 \pm 0.3) \times 10^9 \text{ M}^{-1} \text{ s}^{-1}$, respectively for DMA and DEA (Fig. 4a). k_q for $\text{d}^6\text{-DMA}$ is $(9.0 \pm 0.1) \times 10^9 \text{ M}^{-1} \text{ s}^{-1}$, indicating that there is no deuterium isotope effect. The observed near diffusion-controlled rate constants are consistent with the high excited state redox potential of $\text{NO}_2\text{-OsN}$ (ca. 1.4 V vs. NHE).^{4a} Upon excitation of a mixture of $\text{NO}_2\text{-OsN}$ and DMA in CH_2Cl_2 , a band at ca. 460 nm was observed in the nanosecond transient absorption (ns-TA) spectrum (Fig. 4b), which is similar to that of the $\text{DMA}^{+\cdot}$ cation radical,¹⁰ indicating one-electron oxidation of DMA by $\text{NO}_2\text{-OsN}^*$.

The electronic effects of various *para*-substituents on the aromatic ring of DMA have been investigated by the method of initial rates (R_x), which were obtained from the UV/vis spectral changes of the photoreactions of $\text{NO}_2\text{-OsN}$ with various DMAs (Fig. S12†). The rates were found to be accelerated by electron

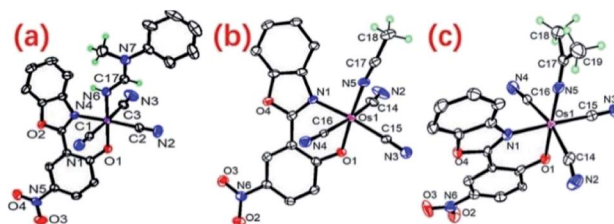


Fig. 3 Molecular structures of 2 (a), 3 (b) and 4 (c). Cations were omitted for simplicity.



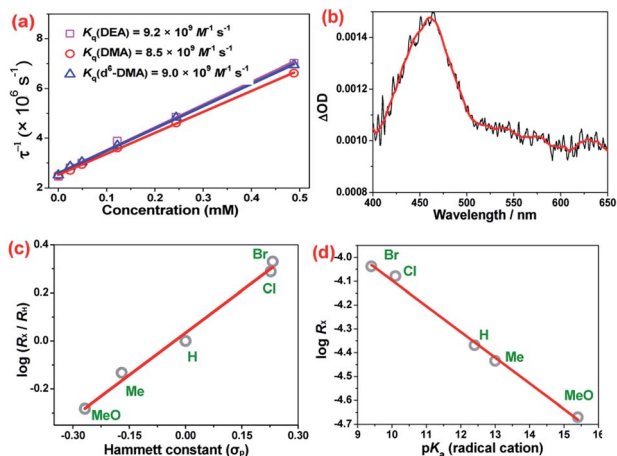


Fig. 4 (a) Stern–Volmer plots for the quenching of $\text{NO}_2\text{-OsN}^*$ ($2.46 \times 10^{-5} \text{ M}$) by DEA, DMA and $\text{d}^6\text{-DMA}$. (b) ns-Transient absorption spectrum of DMA taken immediately after 355 nm laser excitation. (c) Hammett plot of σ_p versus the relative initial rates $\log(R_x/R_H)$ (y -intercept = 0.03 ± 0.01 ; slope = 1.17 ± 0.06 ; $r^2 = 0.989$). (d) Plot of $\log(R_x)$ vs. $\text{p}K_a$ for the radical cation of *para*-substituted DMAs (y -intercept = -3.01 ± 0.08 ; slope = $-(1.08 \pm 0.06) \times 10^{-1}$; $r^2 = 0.992$).

withdrawing groups, and the Hammett plot of $\log(R_x/R_H)$ versus σ_p is linear with a positive ρ value of 1.17 (Fig. 4c). A linear relationship supports a common transition state (TS)/mechanism for the series of reactants, and a positive ρ value indicates that the TS is stabilized by electron-withdrawing substituents. A linear plot was also found for $\log(R_x)$ vs. $\text{p}K_a$ of the radical cations of the DMAs (Fig. 4d and Table S2†).¹¹ These results are consistent with proton transfer from $\text{DMA}^{+\cdot}$ to $\text{NO}_2\text{-Os}^{\text{V}}\text{N}$ in the rate-limiting step, since the acidity of $\text{DMA}^{+\cdot}$ is enhanced by electron-withdrawing substituents.¹² The photoreaction of $\text{NO}_2\text{-OsN}^*$ with *N*-ethyl-*N*-methylaniline was also studied. The result shows that the *N*-demethylation product (72%) is greatly favored over that of *N*-deethylation (4%) (Fig. S13†), which further supports proton transfer as the rate-limiting step, since the acidity of the methyl proton in the radical cation is higher than that of the ethyl protons.¹³

The kinetic isotope effects (KIE) for the *N*-dealkylation reaction of DMA by $\text{NO}_2\text{-OsN}^*$ were determined. Inter-molecular KIE was obtained by competition experiments using equimolar $\text{C}_6\text{H}_5\text{N}(\text{CH}_3)_2$ and $\text{C}_6\text{H}_5\text{N}(\text{CD}_3)_2$ as the substrate (Fig. S14†). A KIE value of 4.0 ± 0.5 was obtained from analysis of the products $\text{C}_6\text{H}_5\text{NHCH}_3$ and $\text{C}_6\text{H}_5\text{NHCD}_3$ by GC/FID and GC/MS. The inter-molecular KIE for amidine formation was also investigated by analysis of the products by ESI/MS, and a KIE of ~ 4.5 was estimated from the ratio of the most intense peaks at m/z 659 and m/z 664 for the protio- and deuterio-osmium(IV) amidine species, respectively, assuming that the spraying and ionization efficiencies of the two ions are similar (Fig. S15†). Intra-molecular KIE was also determined by using 4- $\text{BrC}_6\text{H}_4\text{-N}(\text{CH}_3)(\text{CD}_3)$ as the substrate and a KIE value of 4.9 ± 0.5 was obtained from analysis of the products 4- $\text{BrC}_6\text{H}_5\text{NHCH}_3$ and 4- $\text{BrC}_6\text{H}_5\text{NHCD}_3$ (Fig. S16†). Similar KIE values for the *N*-dealkylation and amidine formation suggest that these two pathways occur *via* a common intermediate.

Proposed mechanism

The experimental results are consistent with an ET/PT mechanism in the *N*-dealkylation of various tertiary amines with $\text{NO}_2\text{-OsN}^*$, as shown in Fig. 5 using DMA as an example. The first step is electron transfer from DMA to $\text{NO}_2\text{-OsN}^*$ to generate $\text{DMA}^{+\cdot}$ and $\text{NO}_2\text{-Os}^{\text{V}}\text{N}$, which occurs at the near diffusion-controlled rate. This step is supported by the observation of the transient $\text{DMA}^{+\cdot}$ species. Rate-limiting proton transfer then occurs from $\text{DMA}^{+\cdot}$ to $\text{NO}_2\text{-Os}^{\text{V}}\text{N}$, followed by rapid N-rebound to give an osmium(IV) amido intermediate, a species that is analogous to the carbinolamine species proposed in cytochrome P_{450} catalyzed *N*-dealkylation of amines,⁶ except that in this case the intermediate amide remains bound to the metal center. The rate-limiting proton transfer step is supported by a large KIE of 4.5, a +ve Hammett ρ value of 1.17, a linear dependence of $\log(R_x)$ on $\text{p}K_a$ and a high preference for *N*-demethylation over *N*-deethylation in the photoreaction of *N*-ethyl-*N*-methylaniline. The osmium(IV) amido species further decomposes *via* two parallel pathways. In pathway A, spontaneous C–N cleavage occurs to give the dealkylated product *N*-methylaniline and an Os(IV) iminato complex, the latter species then undergoes internal redox to afford **1**. In pathway B, the osmium(IV) amido intermediate undergoes H-atom abstraction by another $\text{NO}_2\text{-OsN}^*$ followed by internal redox to give the osmium(III) amidine product. This proposed step is supported by the observed formation of around 1/3 equiv. of $\text{NO}_2\text{-Os}^{\text{III}}\text{NH}_3$: $\text{NO}_2\text{-Os}^{\text{V}}\text{N} + 3\text{H} \rightarrow \text{NO}_2\text{-Os}^{\text{III}}\text{NH}_3$, by UV-vis spectrophotometry. We and others have previously shown that $\text{Os}\equiv\text{N}$ readily abstracts H-atoms from various substrates to give the ammine complex $\text{Os}^{\text{III}}\text{-NH}_3$.^{4a,14} Similar mechanisms are proposed for

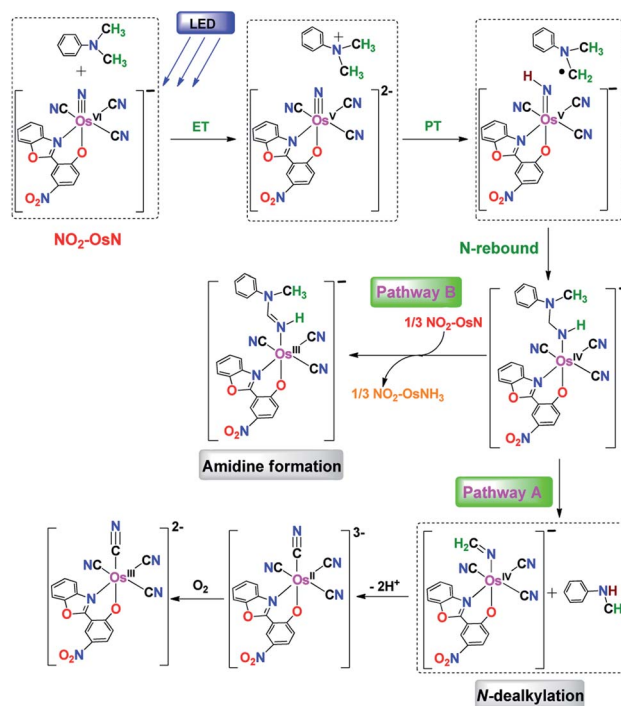


Fig. 5 Proposed mechanism for the reaction of $\text{NO}_2\text{-OsN}^*$ with DMA.



the other substrates (Fig. S17–S19†). Pathway B is much less significant for the other substrates as it does not result in a stable, conjugated amidine ligand as 2.

DFT calculations

Our proposed mechanism for the oxidative dealkylation of tertiary amines by $\text{NO}_2\text{-OsN}$ is also supported by DFT calculations (see ESI, Computational details†). The potential energy surface for the reaction of $\text{NO}_2\text{-Os}^{\text{V}}\text{N}$ with DMA^+ , that is generated from electron transfer between DMA and $\text{NO}_2\text{-OsN}^*$, is shown in Fig. 6; and insets are the structures of the intermediates and transition states. $^3\text{INT1}$ is formed by binding $\text{NO}_2\text{-Os}^{\text{V}}\text{N}$ with DMA^+ via a weak hydrogen bond. A rapid proton transfer from DMA^+ to $\text{NO}_2\text{-Os}^{\text{V}}\text{N}$ occurs via $^3\text{TS1}$ with a barrier height (ΔG_{298}^\ddagger) of $9.8 \text{ kcal mol}^{-1}$, with a simultaneous N-rebound step to generate a stable Os(IV) amido intermediate ($^3\text{INT2}$). The Os–N bond is elongated from 1.739 \AA in $^3\text{INT1}$ to 1.766 \AA in $^3\text{TS1}$ to 1.923 \AA in $^3\text{INT2}$. This is followed by a second proton transfer step from Os(IV) amido to the nitrogen of aniline via $^3\text{TS2}$ ($\Delta G_{298}^\ddagger = -1.8 \text{ kcal mol}^{-1}$) to give an osmium(IV) species ($^3\text{INT3}$) via $^3\text{TS2}$ with a four-member-ring structure. The weak $\text{HN}\dots\text{CH}_2$ bond ($\sim 1.581 \text{ \AA}$) in $^3\text{INT3}$ is then broken to afford the products *N*-methylaniline and osmium(IV) iminato species ($^3\text{INT4}$) via $^3\text{TS3}$; this step is almost barrierless ($0.1 \text{ kcal mol}^{-1}$ relative to $^3\text{INT3}$). Based on our calculations, the rate-determining step is the simultaneous proton transfer and N-rebound step via TS1 .

In conclusion, we have shown that the strongly luminescent osmium(VI) nitrido complex $[\text{Os}^{\text{VI}}(\text{N})(\text{L})(\text{CN})_3]^-$ undergoes facile *N*-dealkylation of aromatic and aliphatic tertiary amines upon irradiation with visible light. We have provided definitive evidence that these reactions occur via an ET/PT mechanism. Our results should contribute to a significant advance in metal nitrido chemistry.

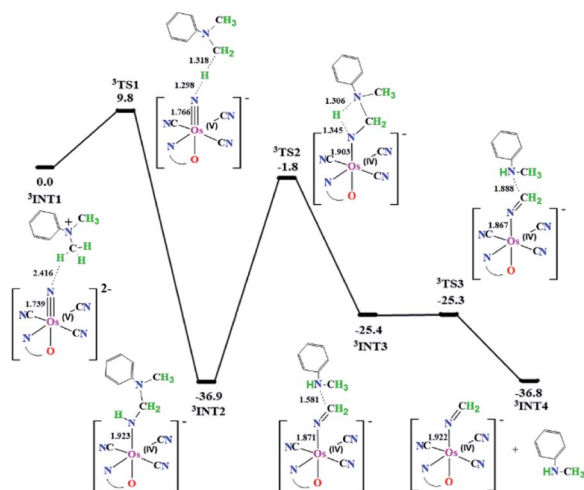


Fig. 6 The potential energy surface for *N*-dealkylation of DMA^+ by $[\text{Os}^{\text{V}}(\text{N})(\text{CN})_3(\text{L})]^{2-}$ in CH_3CN at the B3LYP–D3(BJ)/def2–TZVP level with the PCM solvent effect. Relative 298 K Gibbs free energies in acetonitrile are given in kcal mol^{-1} . Bond lengths are in angstrom (\AA).

Data availability

The datasets supporting this article have been uploaded as part of the ESI.†

Author contributions

J. X. and T.-C. L. designed the experiments, analysed the data and wrote the manuscript. S. M. Y. and W.-L. M. solved the X-ray structures. S.-C. C. and C.-C. K investigated the photophysical properties. M. P., L. J. L. and X. X. J. carried out experiments and analysed the data. Y. P. and K. C. L. did the DFT calculations.

Conflicts of interest

There are no conflicts to declare.

Acknowledgements

This work was supported by the National Natural Science Foundation of China (21771026), the Hubei Provincial Natural Science Foundation of China (2018CFA047), and the Financial support from the Research Grants Council of Hong Kong (CityU 11301618 and N_CityU111/20).

References

- (a) W. A. Nugent and J. M. Mayer, *Metal–Ligand Multiple Bonds*, Wiley-Interscience, New York, 1988; (b) A. Gunay and K. H. Theopold, *Chem. Rev.*, 2010, **110**, 1060–1081; (c) M. Costas, M. P. Mehn, M. P. Jensen and L. Que Jr, *Chem. Rev.*, 2004, **104**, 939–986; (d) M. Guo, T. Corona, K. Ray and W. Nam, *ACS Cent. Sci.*, 2019, **5**, 13–28.
- (a) T. J. Meyer and M. H. V. Huynh, *Inorg. Chem.*, 2003, **42**, 8140–8160; (b) W. L. Man, W. W. Y. Lam and T. C. Lau, *Acc. Chem. Res.*, 2014, **47**, 427–439; (c) M. H. V. Huynh, T. J. Meyer, M. A. Hiskey and D. L. Jameson, *J. Am. Chem. Soc.*, 2004, **126**, 3608–3615; (d) A. G. Maestri, K. S. Cherry, J. J. Toboni and S. N. Brown, *J. Am. Chem. Soc.*, 2001, **123**, 7459–7460; (e) M. R. McCarthy, T. J. Crevier, B. Bennett, A. Dehestani and J. M. Mayer, *J. Am. Chem. Soc.*, 2000, **122**, 12391–12392; (f) T. J. Crevier, B. K. Bennett, J. D. Soper, J. A. Bowman, A. Dehestani, D. A. Hrovat, S. Lovell, W. Kaminsky and J. M. Mayer, *J. Am. Chem. Soc.*, 2001, **123**, 1059–1071; (g) A. Dehestani, W. Kaminsky and J. M. Mayer, *Inorg. Chem.*, 2003, **42**, 605–611; (h) J. H. Xie, W. L. Man, C. Y. Wong, X. Y. Chang, C. M. Che and T. C. Lau, *J. Am. Chem. Soc.*, 2016, **138**, 5817–5820; (i) W. L. Man, W. W. Y. Lam, H. K. Kwong, S. M. Yiu and T. C. Lau, *Angew. Chem., Int. Ed.*, 2012, **51**, 9101–9104; (j) W. L. Man, W. W. Y. Lam, S. M. Yiu, T. C. Lau and S. M. Peng, *J. Am. Chem. Soc.*, 2004, **126**, 15336–15337; (k) S. B. Muñoz III, W. T. Lee, D. A. Dickie, J. J. Scepaniak, D. Subedi, M. Pink, M. D. Johnson and J. M. Smith, *Angew. Chem., Int. Ed.*, 2015, **54**, 10600–10603; (l) J. J. Scepaniak, J. A. Young, R. P. Bontchev and J. M. Smith, *Angew. Chem., Int. ed.*, 2009, **48**, 3158–3160; (m) J. J. Scepaniak, C. S. Vogel,



- M. M. Khusniyarov, F. W. Heinemann, K. Meyer and J. M. Smith, *Science*, 2011, **33**, 1049–1052; (n) M. Baya, J. Houghton, D. Konya, Y. Champouret, J. C. Daran, K. Q. AlmeidaLeñero, L. Schoon, W. P. Mul, A. B. vanOort, N. Meijboom, E. Drent, A. G. Orpen and R. Poli, *J. Am. Chem. Soc.*, 2008, **130**, 10612–10624; (o) T. A. Betley and J. C. Peters, *J. Am. Chem. Soc.*, 2004, **12**, 6252–6254; (p) N. B. Thompson, M. T. Green and J. C. Peters, *J. Am. Chem. Soc.*, 2017, **13**, 15312–15315.
- 3 (a) R. M. Clarke and T. Storr, *J. Am. Chem. Soc.*, 2016, **138**, 15299–15302; (b) M. Keener, M. Peterson, R. H. Sánchez, V. F. Oswald, G. Wu and G. Ménard, *Chem.–Eur. J.*, 2017, **23**, 11479–11484; (c) W.-L. Man, T.-M. Tang, T.-W. Wong, T.-C. Lau, S.-M. Peng and W.-T. Wong, *J. Am. Chem. Soc.*, 2004, **126**, 478–479; (d) W. L. Mishina, G. Chen and S. M. Yiu, *Dalton Trans.*, 2010, **39**, 11163–11170; (e) D. C. Ware and H. Taube, *Inorg. Chem.*, 1991, **30**, 4605–4610.
- 4 (a) J. Xiang, X. X. Jin, Q. Q. Su, S. C. Cheng, C. C. Ko, W. L. Man, M. Y. Xue, L. L. Wu, C. M. Che and T. C. Lau, *Commun. Chem.*, 2019, **2**, 40; (b) L.-J. Luo, Q.-Q. Su, S.-C. Cheng, J. Xiang, W.-L. Man, W.-M. Shu, M.-H. Zeng, S.-M. Yiu, C.-C. Ko and T.-C. Lau, *Inorg. Chem.*, 2020, **59**, 4406–4413; (c) J. Xiang, W. L. Man, S. M. Yiu, S. M. Peng and T. C. Lau, *Chem.–Eur. J.*, 2011, **17**, 13044–13051; (d) J. Xiang, Q. Wang, S. M. Yiu, W. L. Man, H. K. Kwong and T. C. Lau, *Inorg. Chem.*, 2016, **55**, 5056–5061; (e) J. Xiang, Q. Wang, S. M. You and T. C. Lau, *Inorg. Chem.*, 2017, **56**, 2022–2028.
- 5 (a) M. Sono, M. P. Roach, E. D. Coulter and J. H. Dawson, *Chem. Rev.*, 1996, **96**, 2841–2888; (b) Y. Mishina and C. He, *J. Inorg. Biochem.*, 2006, **100**, 670–678.
- 6 (a) H. C. Aspinall, J. Bacsá, A. C. Jones, J. S. Wrench, K. Black, P. R. Chalker, P. J. King, P. Marshall, M. Werner, H. O. Davies and R. Odedra, *Inorg. Chem.*, 2011, **50**, 11644–11652; (b) A. Barbieri, M. De Gennaro, S. Di Stefano, O. Lanzalunga, A. Lapi, M. Mazzonna, G. Olivo and B. Ticconi, *Chem. Commun.*, 2015, **51**, 5032.
- 7 (a) F. P. Guengerich, C. H. Yun and T. L. Macdonald, *J. Biol. Chem.*, 1996, **271**, 27321–27329; (b) C. Li, W. Wu and K. B. Cho, *Chem.–Eur. J.*, 2009, **15**, 8492–8503.
- 8 Q.-Q. Su, K. Fan, X.-D. Huang, J. Xiang, S.-C. Cheng, C.-C. Ko, L.-M. Zheng, M. Kurmood and T.-C. Lau, *Dalton Trans.*, 2020, **49**, 4084–4092.
- 9 (a) P. J. Bailey and S. Pace, *Coord. Chem. Rev.*, 2001, **214**, 91–141; (b) T. Chlupatý and A. Růžička, *Coord. Chem. Rev.*, 2016, **314**, 103–113; (c) J. Xiang, Q.-Q. Su, L.-J. Luo and T.-C. Lau, *Dalton Trans.*, 2019, **48**, 11404–11410.
- 10 H. Kandori, K. Kemnitz and K. Yoshihara, *J. Phys. Chem.*, 1992, **96**, 8042–8048.
- 11 (a) A. Barbieri, M. De Gennaro, S. Di Stefano, O. Lanzalunga, A. Lapi, M. Mazzonna, G. Olivo and B. Ticconi, *Chem. Commun.*, 2015, **51**, 5032–5035; (b) E. Baciocchi, M. F. Gerini, O. Lanzalunga, A. Lapi, M. G. L. Piparo and S. Mancinelli, *Eur. J. Org. Chem.*, 2001, **2001**, 2305–2310; (c) M. Jonsson, D. D. M. Wayner and J. Lusztyk, *J. Phys. Chem.*, 1996, **100**, 17539–17543; (d) V. D. Parker and M. Tilset, *J. Am. Chem. Soc.*, 1991, **113**, 8778–8781; (e) G. W. Dombrowski, J. P. Dinnocenzo, S. Farid, J. L. Goodman and I. R. Gould, *J. Org. Chem.*, 1999, **64**, 427–431; (f) F. G. Bordwell, J.-P. Cheng and J. A. Harrelson Jr, *J. Am. Chem. Soc.*, 1988, **110**, 1229–1231; (g) D. D. M. Wayner and V. D. Parker, *Acc. Chem. Res.*, 1993, **26**, 287–294.
- 12 S. Sumalekshmy and K. R. Gopidas, *Chem. Phys. Lett.*, 2005, **413**, 294–299.
- 13 (a) O. Okazaki and F. P. Guengerich, *J. Biol. Chem.*, 1993, **268**, 1546–1552; (b) K. Nehru, M. S. Seo, J. H. Kim and W. Nam, *Inorg. Chem.*, 2007, **46**, 293–298.
- 14 G. Berger, A. Wach, J. Sá and J. Szlachetko, *Inorg. Chem.*, 2021, **60**, 6663–6671.

